Electronic Supplementary Material (ESI) for Journal of Materials Chemistry A.

Supporting information

A mechanical-optical coupling design on solar and thermal radiation modulation for thermoregulation

Na Guo [1], Changmin Shi [2,*], Brian W. Sheldon[2], Hongjie Yan [1], Meijie Chen [1,*]

[1] School of Energy Science and Engineering, Central South University, Changsha 430001, China

[2] School of Engineering, Brown University, Providence, RI 02906, USA.

* Corresponding Authors. chenmeijie@csu.edu.cn (M. Chen); changmin_shi@brown.edu (C. Shi)

Section S1 Net power calculation

Net cooling power $P_{cooling}$ or heating power $P_{heating}$ was calculated based energy balance equation when the ambient temperature T_{amb} is equal to the coating temperature T_c:

$$P_{cooling} = P_{rad} - P_{sol} - P_{atm} \quad (1)$$

$$P_{heating} = P_{sol} + P_{atm} - P_{rad} \quad (2)$$

where P_{sol} is the absorbed solar radiation. P_{atm} is the absorbed radiation power from the atmosphere. P_{rad} is the radiation power of the coating.

P_{sol} can be calculated from the following equation:

$$P_{sol}(T_c) = \alpha(\lambda,T_c) I_{sol}(\lambda) d\lambda \quad (3)$$

where λ is the wavelength. $\alpha(\lambda,T_c)$ is the spectral absorptance of the coating. $I_{sol}(\lambda)$ is the solar intensity.

P_{atm} can be calculated from the following equation:

$$P_{atm}(T_{amb}) = \int \varepsilon_{atm}(\lambda)\alpha(\lambda) I_B(\lambda,T_{amb}) d\lambda \quad (4)$$

where $\varepsilon_{atm}(\lambda)$ is the emittance of the atmosphere. $\alpha(\lambda)$ is the spectral absorptance of the SEBS@Ag film. $I_B(\lambda,T_{amb})$ is the spectral radiation intensity of the blackbody (the temperature is the same as the ambient temperature), which can be calculated according to Planck's law:

$$I_B(\lambda,T) = \frac{c_1 \lambda^{-5}}{e^{c_2/(\lambda T)} - 1} \quad (5)$$

where c_1 is the first radiation constant with the value of 3.7419×10^{-16} W·m^2, and c_2 is the second radiation constant with the value of 1.4388×10^{-2} m·K.

P_{rad} can be calculated from the Stefan-Boltzmann formula:

$$P_{rad}(T) = \int \alpha(\lambda) I_B(\lambda,T_c) d\lambda \quad (6)$$

where $I_B(\lambda,T_c)$ is the spectral radiation intensity of the blackbody and the temperature is the same as the coating.

The average solar reflectance and transmittance can be defined as:

$$\bar{R}_{sol} = \frac{\int_{0.3\mu m}^{2.5\mu m} R(\theta,\lambda) I_{sol}(\lambda) d\lambda}{\int_{0.3\mu m}^{2.5\mu m} I_{sol}(\lambda) d\lambda} \quad (7)$$

$$\bar{\tau}_{sol} = \frac{\int_{0.3\mu m}^{2.5\mu m} \tau(\theta,\lambda) I_{sol}(\lambda) d\lambda}{\int_{0.3\mu m}^{2.5\mu m} I_{sol}(\lambda) d\lambda} \quad (8)$$

The average thermal reflectance and transmittance in λ = 8 – 13 μm (i.e., the atmospheric transparent window) are usually used to determine the radiative cooling performance as follows:

$$\bar{R}_{LWIR} = \frac{\int_{8\mu m}^{13\mu m} I_B(\lambda,T_c) R(T_c,\lambda) d\lambda}{\int_{8\mu m}^{13\mu m} I_B(\lambda,T_c) d\lambda} \quad (9)$$

$$\bar{\tau}_{LWIR} = \frac{\int_{8\mu m}^{13\mu m} I_B(\lambda,T_c) \tau(T_c,\lambda) d\lambda}{\int_{8\mu m}^{13\mu m} I_B(\lambda,T_c) d\lambda} \quad (10)$$

Section S2: Energy-saving calculation

A conventional rectangular building (12 m x 10 m x 4 m) was built, the roof area of the building was A = 120 m^2 in Figure 3e. The ASHRAE (American Society of Heating, Refrigerating, and Air-Conditioning Engineers) database was used for material parameters. The walls of the building were made of stucco, concrete, wall insulation, and gypsum, thermal conductivity was 0.69, 1.73, 0.04, and 0.16 W m^{-1} K^{-1}, respectively. The exterior doors were made of insulation board and metal surface, and thermal conductivity was 0.03 and 45.30 W m^{-1} K^{-1}, respectively. The stretchable SEBS@Ag film covered the roof glass. The annual meteorological data, including hourly temperature, solar radiation intensity, and outdoor humidity, can be obtained from the weather database in EnergyPlus. HVAC systems were set up in the room to calculate the energy consumption of the building. When the indoor temperature was below 20 °C, it heated the room, and when above 28 °C, it cooled the room. The HVAC systems were turned on from 8 a.m. to 5 p.m., excluding two weekends per week, and the indoor personnel density was 2 m^2 / person, excluding the impact of the use of other electrical appliances.

Section S3: SEBS intrinsic absorption coefficient calculation

The transmittance of a SEBS film without a metal layer at the bottom can be expressed according to Beer-Lambert law:

$$\tau = (1 - R_1)^2 e^{-\mu_p l} = (1 - R_1)^2 e^{-\mu_p d} \quad (11)$$

where R_1 is the reflectance of the SEBS/air interface (Fresnel reflection). μ_p is the absorption coefficient. l is the length of the light path, d is the thickness of the SEBS film.

The total reflectance R of the surface and bottom reflectance is calculated by the following formula:

$$R = R_1 + R_1(1 - R_1)^2 e^{-2\mu_p l} \quad (12)$$

The refractive index can be calculated by the following formula:

$$n' = n + ik \quad (13)$$

R_1 can also be calculated by the Fresnel equation:

$$R_1 = \left| \frac{n_{SEBS} - n_{air}}{n_{SEBS} + n_{air}} \right|^2 \quad (14)$$

$$\mu_p = \frac{4\pi k}{\lambda_0} \quad (15)$$

where n is the real part of the refraction index, k is the imaginary part of the index of refraction (extinction coefficient). n_{SEBS} and n_{air} are the refractive index of SEBS and air in the mid-infrared band, take the n_{air} = 1, λ_0 is the wavelength.

According to Kirchhoff's law: α can be derived as:

$$\alpha = 1 - R - \tau = (1 - R_1) - (1 - R_1)^2 e^{-\mu_p d} - R_1(1 - R_1)^2 e^{-2\mu_p l} \quad (16)$$

Section S4: Spectral modulation calculation

Assuming that SEBS@Ag film has the original length l and the stretched length becomes l', then its change in length $\Delta l = l' - l$, and the stretch strain ε is the ratio of the change Δl to the original length l, as follows:

$$\varepsilon = \frac{\Delta l}{l} \tag{17}$$

To simplify the calculation model, the volume of SEBS film, the surface area of Ag film, and the width of the film did not change during the stretching process.

$$V = lbh \tag{18}$$

where V, l, b, and h are the volume, length, width, and thickness of SEBS film, respectively. During the stretching process, its volume does not change, so there is the following equation:

$$V = lbh = (l + \varepsilon l)bh' \tag{19}$$

Therefore, the thickness after stretching is:

$$h' = \frac{1}{1+\varepsilon}h \tag{20}$$

When the strain was 0 %, 100 %, and 200 %, the thickness would be $1h$, $1/2h$, and $1/3h$ (**Figure S7**). Due to the bottom Ag layer being highly reflective, mid-infrared absorption occurs twice where the Ag is covered. Therefore, the effective intrinsic absorption thickness after stretching is:

$$h'' = \left(\frac{l}{l+\varepsilon l} \times 2 + \frac{\varepsilon l}{l+\varepsilon l} \times 1\right)h' = \frac{(2+\varepsilon)}{(1+\varepsilon)^2}h \tag{21}$$

The effective intrinsic absorption thickness of SEBS film was $2h$, $3/4h$, and $4/9h$ under strain of 0 %, 100 %, and 200 % (Figure S4). Solar reflectance was related to the area occupied by the underlying Ag, so the solar reflectance after stretching is:

$$R' = \left(\frac{l}{l+\varepsilon l}\right)R = \frac{1}{1+\varepsilon}R \tag{22}$$

When the strain was 100 % and 200 %, the solar reflectance would become 1/2 and 1/3 of the original release state.

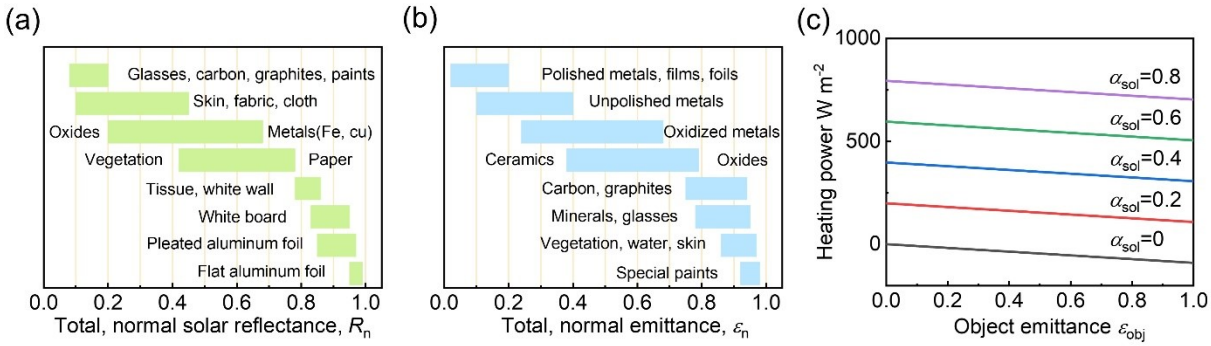

Figure S1 The total, normal (a) solar reflectance and (b) thermal emittance of some common objects. (c) Under the ideal condition of SEBS@Ag film stretching state, when the solar absorptance of the lower object is different, the heating power of the whole system changes with the thermal emittance of the object.

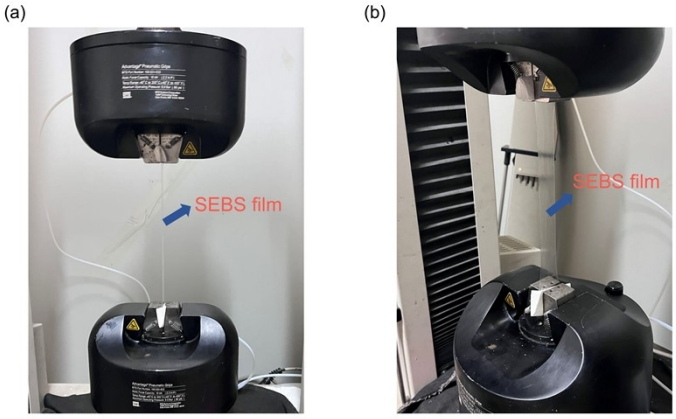

Figure S2 SEBS film stretching physical pictures.

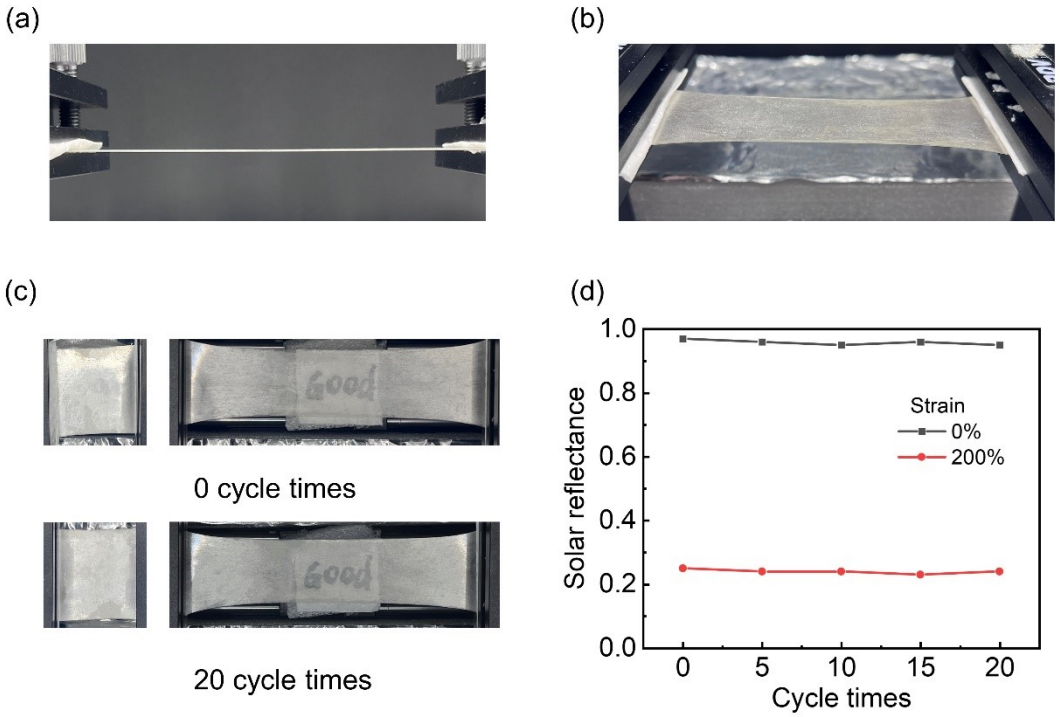

Figure S3 (a) and (b) Optical images of SEBS@Ag film in the stretching process. Optical image (c) and solar reflectance (d) after multiple stretching cycle times.

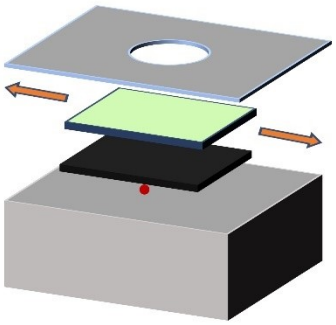

Figure S4 Mechanical stretching diagram of outdoor experimental SEBS@Ag film.

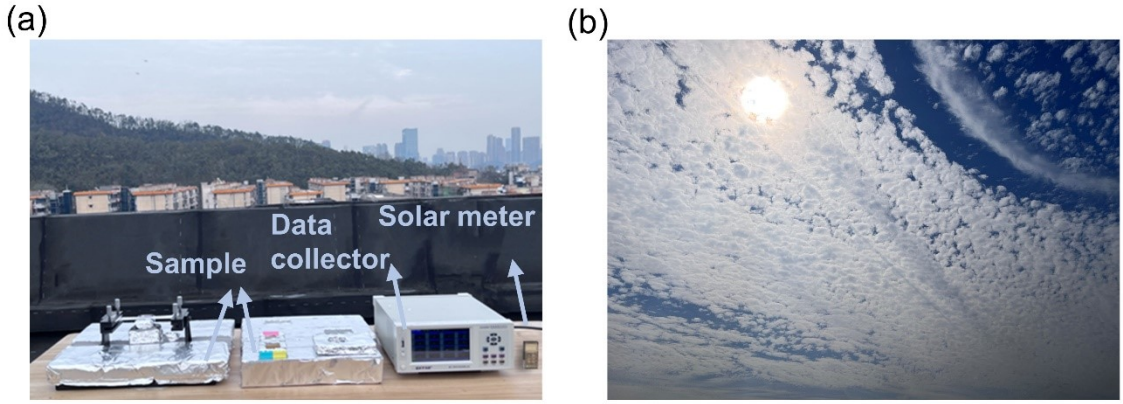

Figure S5 (a) Outdoor test diagram. (b) Cloudy sky in the afternoon of 2024-03-12.

Figure S6 Map of 18 typical cities around the world.

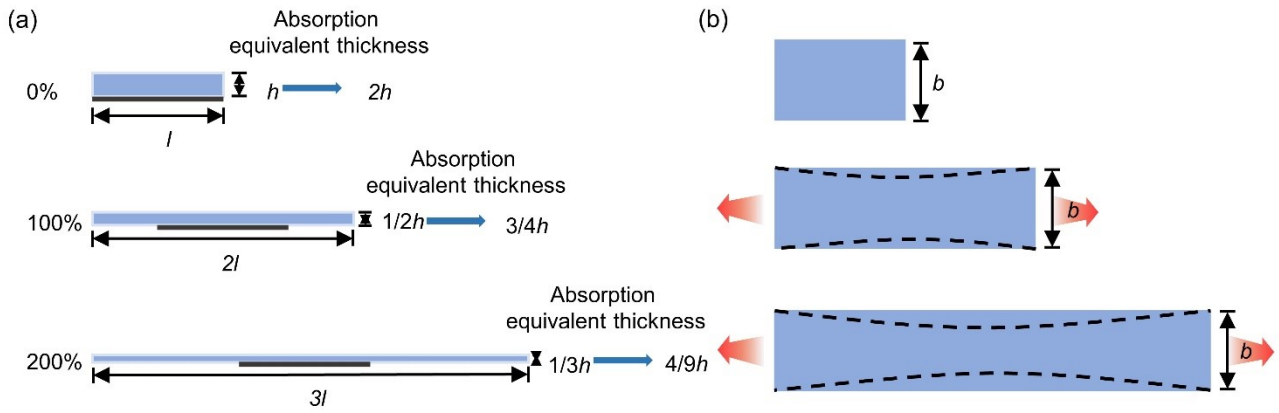

Figure S7 Theoretical analysis of stretch strain. (a) The side and (b) top view of the film stretches (The dashed line shows the actual width change).

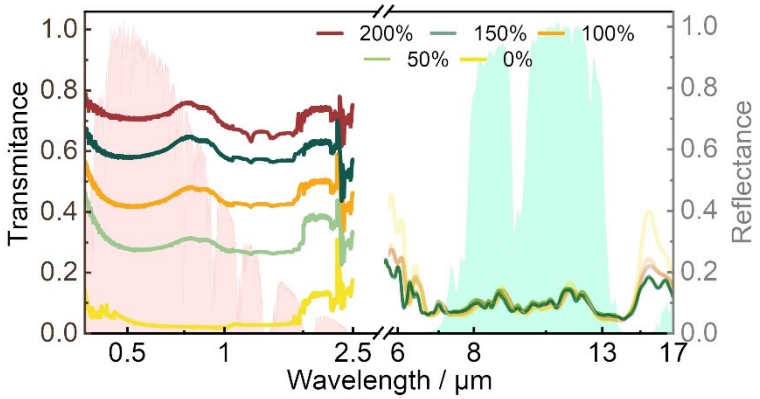

Figure S8 Changes of solar reflectance and mid-infrared transmittance of SEBS@Ag film (The thickness ~ 300 μm) at 0 %, 50 %, 100 %, 150 % and 200 % strain.

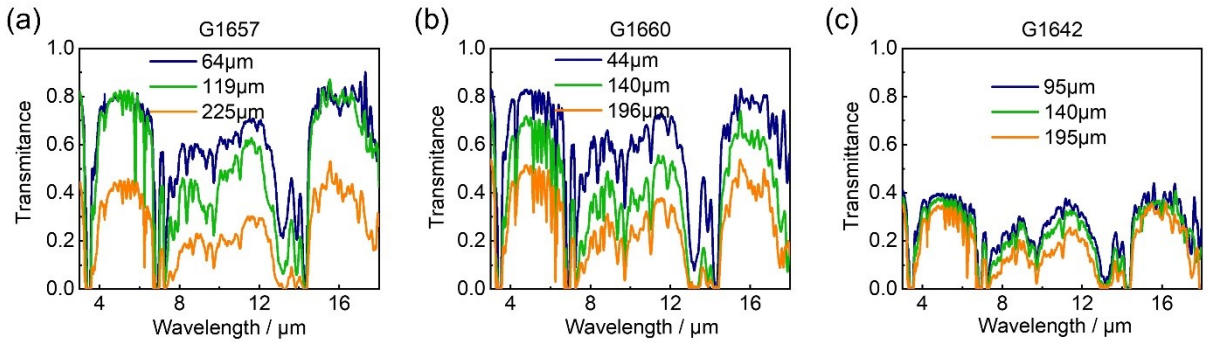

Figure S9 Spectral transmittance under different thicknesses for (a) G1657 SEBS films, (b) G1660 SEBS films, and (c) G1642 SEBS films.

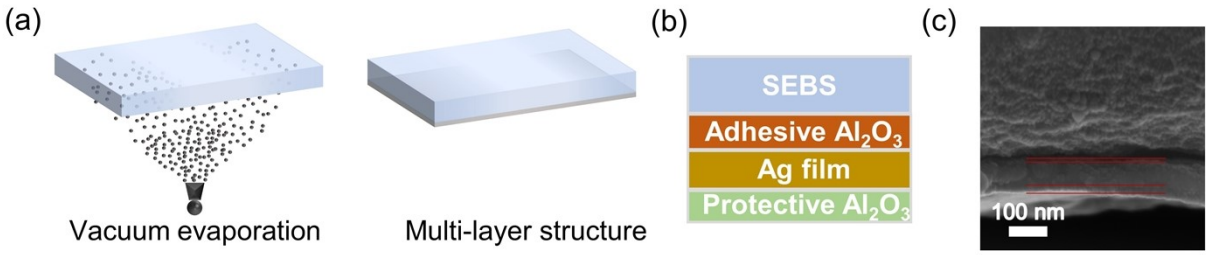

Figure S10 Multilayer structure of SEBS@Ag film. (a) Vacuum evaporation diagram of the SEBS@Ag film during silver plating. (b) Schematic diagram of the layered structure of the SEBS@Ag film. (c) SEM image of SEBS@Ag film cross-section stratification structure.

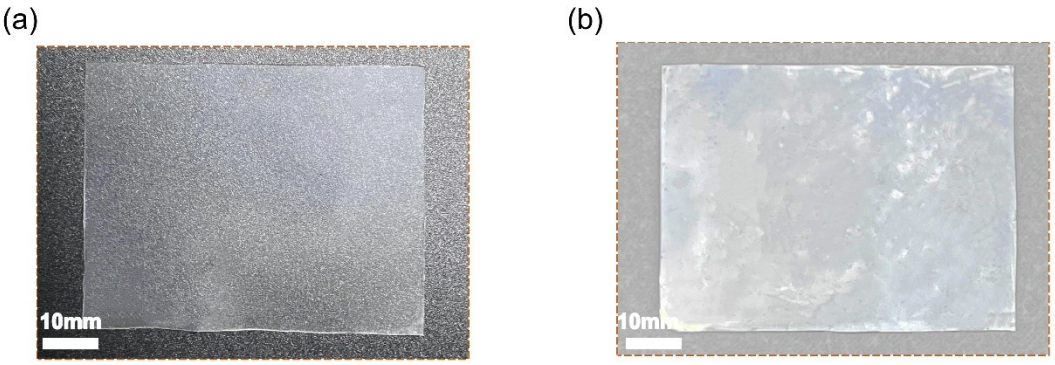

Figure S11 Optical images of the (a) SEBS film and (b) SEBS@Ag film.

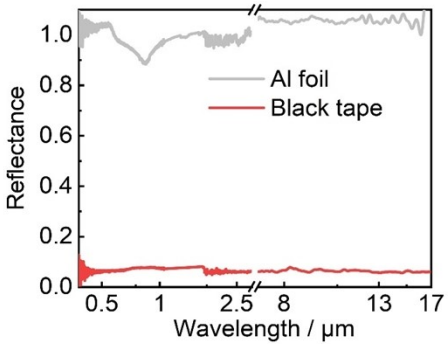

Figure S12 Full spectral reflectance of Al foil and black tape.

Table S1 Comparison and summary of various thermal radiative regulations.

Category	Material	Modulation	Advantage	Remark
Electrochromic	Micro wrinkle TiO_2 Films [1]	0.79(ΔT_{sol})	Low-cost, durable, high performance	2018
	Reversible electro-deposition [2]	0.76(ΔT_{vis})	Fast response, excellent uniformity	2021
	Kirigami-enabled electrochromic thin film[3]	0.27($\Delta \varepsilon_{LWIR}$)	Programmable personalized thermoregulation	2022
	Electrodepositing Cu on the transparent electrode [4]	0.85($\Delta \varepsilon_{MIR}$)	Fast response speed	2022
Thermochromic	The hydrogel-derived liquid [5]	0.90(ΔT_{vis}), 0.68(ΔT_{sol})	Easy fabrication, good uniformity, scalability	2020
	Thermo-Responsive Hydrogel [6]	0.91(ΔT_{vis}), 0.82(ΔT_{sol})	Good indoor temperature regulation ability and stability	2023
	$VO_2/MgF_2/W$ [7]	0.58($\Delta \varepsilon_{MIR}$)	Without any extra energy input	2018
	CaF_2/VO_2 Core−shell microsphere[8]	0.36($\Delta \varepsilon_{MIR}$)	Self-regulating, completely passive, flexible	2021
	$Al_2O_3/VO_2/Al_2O_3/Al$ [9]	0.50($\Delta \varepsilon_{MIR}$)	Efficient energy harvesting	2022
Mechanochromic	silica particles embedded in bulk elastomeric PDMS [10]	~0.60(ΔT_{vis})	Low-cost, facile, highly robust	2015

	PDMS layer embedded with nano-particles: SiC, Si_3N_4, and BN [11]	0.64($\Delta\varepsilon_{MIR}$)	Low-cost, simple preparation process	2020
	Multi-layered structure cephalopod-inspired system [12]	0.32($\Delta\varepsilon_{MIR}$)	Instantaneous response, feasibility	2021
	Wrinkles and cracks in PEDOT: PSS and PDMS [13]	0.55(ΔT_{sol}), 0.25(ΔR_{MIR})	Clever structure, simple preparation process	2022
	Dynamic dual-mode thermal-management device [14]	0.38($\Delta\alpha_{sol}$), 0.67($\Delta\varepsilon_{MIR}$)	Environmentally friendly, zero-energy	2022
	Multi-layer structure SEBS@Ag film	0.72(ΔT_{sol}), 0.3($\Delta\varepsilon_{LWIR}$)	Environmentally friendly, large modulation range	This work

ΔT_{sol} and ΔT_{vis} represent the transmittance modulation in the solar spectrum and visible spectrum.

$\Delta\alpha_{sol}$, $\Delta\varepsilon_{LWIR}$, and $\Delta\varepsilon_{MIR}$ represent the solar absorptance modulation, thermal emittance modulation in the atmosphere's long-wave infrared transmission window (8 – 13 μm), and the mid-infrared spectrum (2.5 – 30 μm).

ΔR_{sol}, ΔR_{LWIR}, and ΔR_{MIR} represent the reflectance modulation in the solar spectrum, the atmosphere's long-wave infrared transmission window (8 – 13 μm), and the mid-infrared spectrum (2.5 – 30 μm).

.

Table S2 Annual total energy consumption comparison data.

City	Canberra	Los angles	Mexico City	Toronto	Washington D.C.	Buenos Aires	New Delhi	Lhasa	Beijing
SEBS@Ag film covered standard glasses / GJ	46.4	36.0	34.8	106.4	81.4	34.2	50.8	70.0	80.7
Standard glass / GJ	82.6	79.5	74.0	142.7	117.3	75.2	117.2	87.9	113.5
Energy saving (vs. standard glass)	43.8%	54.7%	53.0%	25.4%	30.6%	54.5%	56.7%	20.4%	28.9%
City	Harbin	Shanghai	Tokyo	Reykjavik	London	Rome	Cairo	Cape Town	Moscow
SEBS@Ag film covered standard glasses / GJ	146.5	53.5	64.2	114.1	107.6	50.3	47.0	35.1	121.6
Standard glass / GJ	184.4	84.8	88.5	144.9	143.1	91.5	102.8	77.9	155.6
Energy saving (vs. standard glass)	20.6%	36.9%	27.5%	21.3%	24.8%	45.0%	54.3%	54.9%	21.9%

References

1. Shrestha, M. Asundi, A. Lau, G. K. Smart window based on electric unfolding of microwrinkled TiO2 nanometric films. *ACS Photonics*. **5**, 3255–3262 (2018).
2. Strand, MT. Hernandez, TS. Danner, MG. Yeang, AL. Jarvey, N. Barile, CJ. McGehee, MD. Polymer inhibitors enable >900 cm^2 dynamic windows based on reversible metal electrodeposition with high solar modulation. *Nat. Energy*. **6**, 546–554 (2021).
3. Chen, TH. Hong, YY. Fu, CT. Nandi, AK. Xie, WR. Yin, J. Hsu, PC. A kirigami-enabled electrochromic wearable variable emittance (WeaVE) device for energy- efficient adaptive personal thermoregulation. *PANS nexus*. **2**, 6 (2023).
4. Sui, C. Pu, J. Chen, TH. Lai, YT. Rao, YF. Li, X. L, J. Viswanathan, V. Hsu, PC. Aqueous mid-infrared electrically switchable opaque building envelopes for all-season radiative thermoregulation. *Research Square*. (2022).
5. Zhou, Y. Wang, S. Peng, J. Tan, Y. Li, C. Boey, F. Long, Y. Liquid thermo-responsive smart window derived from hydrogel. *Joule*. **4**, 2458–2474 (2020).
6. Wang, K. Chen, G. Weng, S. Hou, L. Ye, D. Jiang, X. Thermo-responsive poly(N-isopropylacrylamide)/hydroxypropylmethyl cellulose hydrogel with high luminous transmittance and solar modulation for smart windows. *ACS Appl. Mater. Interfaces.* **15**, 3, 4385-4397 (2023).
7. Ono, M. Takata, M. Shirata, M. Yoshihiro, T. Tani, T. Naya, M. Saiki, T. Self-adaptive control of infrared emissivity in a solution-processed plasmonic structure. *Opt. Express*. **29**, 36048 (2021).
8. Wu, X. Yuan, L. Weng, X. Qi, L. Wei, B. He W. Passive smart thermal control

coatings incorporating CaF_2/VO_2 core-shell microsphere structures. *Nano Lett.* **21**, 3908–3914 (2021).

9. Ao, XZ. Li, BW. Zhao, B. Hu, MK. Ren, H. Yang, HL. Liu, J. Cao, JY. Feng, JS. Yang, YJ. Qi, ZM. Li, LB. Zou, CW. Pei, G. Self-adaptive integration of photothermal and radiative cooling for continuous energy harvesting from the sun and outer space. *Proc. Natl. Acad. Sci. U. S. A.* **119**, e2120557119 (2022).
10. Ge, D. Lee, E. Yang, L. Cho, Y. Li, M. Gianola, D. Yang, S. A robust smart window : reversibly switching from high transparency to angle-independent structural color display. *Advanced Materials*. **27**, 15, 2489–2495 (2015).
11. Liu, XJ. Tian, YP. Chen, FQ. Ghanekar, A. Antezza, M. Zheng, Y. Continuously variable emission for mechanical deformation induced radiative cooling. *Commun. Mater*. **1**, 95 (2020).
12. Zeng, SS. Shen, KY. Liu, Y. Chooi, AP. Smith, AT. Zhai, SH. Chen, Z. Sun, LY. Dynamic thermal radiation modulators via mechanically tunable surface emissivity. *Mater. Today.* **45**, 44–53 (2021).
13. Zhou, ZG. Fang, YS. Wang, X. Yang, EQ. Liu, R. Zhou, XS. Huang, Z. Yin, HZ. Zhou, J. Hu, B. Synergistic modulation of solar and thermal radiation in dynamic energy-efficient windows. *Nano Energy.* **93**, 106865 (2022).
14. Zhang, Q. Lv, YW. Wang, YF. Yu, SX. Li, CX. Ma, RJ. Chen, YS. Temperature-dependent dual-mode thermal management device with net zero energy for year-round energy saving. *Nat. Commun.* **13**, 4874 (2022).